Surface Superconductivity of the Ti-22 at.% Nb Alloy

V. R. Karasik, N. G. Vasil'ev, and V. S. Vysotskii

P. N. Lebedev Physics Institute, USSR Academy of Sciences

Submitted November 24, 1971

Zh. Eksp. Teor. Fiz. 62, 1818–1826 (1972)

The effect of the structural states of the alloy Ti-22 at.% Nb on its critical temperature, resistivity, critical field strengths H_{c2} and H_{c3} and critical current density of surface superconductivity near T_c is investigated. An anomalous temperature dependence of the ratio H_{c3}/H_{c2} is observed. The dependence of the surface superconductivity critical current and the critical field strength H_{c3} on the angle between the plane of the sample and the direction of the external magnetic field is studied.

A connection was established in[1,2] between the structural states of the alloy Ti-22 at.% Nb and the behavior of the bulk critical currents in the mixed state. Measurements of $j_{cr\perp}(H, T)$, $j_{cr\parallel}(H, T)$, the magnetic moment connected with the induced currents, and the anisotropy of j_{cr} relative to the angle between the current and the field, have all shown that the character of the dependence $j_{cr}(H, t)$ and the value of the critical current are determined by the relation between the diameter of the Abrikosov vortex and the linear dimensions of the particles of the ω and α phases, which appear in the alloy Ti-22 at.% Nb as effective pinning points.

It is of interest to make clear whether these regularities extend to the case of surface super conductivity, when the vortex structure appears as the consequence of the presence of an angle between the magnetic field and the surface of the sample, and when its period is determined by the relation[3] [1)]

$$d = (\Phi_0 / H \sin \theta)^{1/2}. \tag{1}$$

Here θ is the angle between the plane of the sample and the direction of the external field, and $\Phi_0 = 2 \times 10^{-7}$ G-cm^2 is the magnetic flux quantum.

It is also of interest to establish the correlation between the structural states of the alloy and its parameters, such as H_{c2}, H_{c3}, κ, and the ratio H_{c3}/H_{c2} near T_c.

1. METHOD OF MEASUREMENT AND SAMPLE PREPARATION

To obtain temperatures $4.2°K < T < 10°K$, we used an inverted dewar made of stainless tubing.[5] The temperature was stabilized with an accuracy $\pm 0.001°K$. A carbon resistance thermometer and the sample were in good thermal contact with a copper block.

The measurements were carried out on wires of diameter 0.6 mm and strips of length 7–15 mm, width 2 mm and thickness 90 μ. To improve the surface, the samples were polished mechanically before thermal treatment, by means of abrasives with grain dimensions from 10 to 1 μ. They were then electropolished in a solution consisting of six parts nitric acid, two parts fluoric acid, and two parts sulfuric acid. The

electropolished samples, with mirror-smooth surfaces, were recrystallized at a temperature of 800°C for 1 hour. After recrystallization, the ampule with the samples was cooled in water. The recrystallized samples were of single phase. Then, aging was carried out at a temperature of 390° or 500°C. During this aging, the ω and α phases are separated out from the β solid solution at these respective temperatures. The structure of the alloy was investigated by the methods of x-ray analysis and transmission electron microscopy with the application of microdiffraction.[6,7] The phase composition of the samples is given in Table I.

The samples, treated at a temperature of 390°C, contained precipitates of hexagonal ω phase in the form of ellipsoids. The mean size of the ω particles in this series ranges from 50 Å for sample No. 1 to 440 $\times$ 160 Å for sample No. 4. In samples Nos. 5—10, needle-shaped particles of the α phase are precipitated.

To decrease the contact resistance, the current and potential contacts were built up on the sample with pure indium by means of ultrasonic soldering. The value of the transition resistance amounted to 10^{-7} ohm, which is much less than the resistance of the sample in the normal state, which is of the order of $\sim 10^{-2}$ ohm. As a critical current of the surface superconductivity, we applied a current which created the minimum experimentally detectable drop in potential U_0 between the potential contacts, equal to 4×10^{-8} V.

The critical field H_{c2} was determined by measuring the magnetic moment by the ballistic method (see Fig. 1a). To determine the critical field H_{c3}, we used the curves of the reconstructed resistance (see Fig. 1b): when the value of the transport current is sufficiently small, the transition of the sample to the normal state is virtually complete in the field H_{c3}. For the field value H_{c3}, we used that value for which the resistance of the samples was equal to $0.99R_n$.

The critical temperature T_c was determined at a

[1)] As was shown in [4], in view of the non-ideal nature of the experimental conditions—roughness of the surface, inaccurate mounting of the sample, inhomogeneity of the magnetic field, etc.—under real conditions, an angle always exists between the field and the surface and, consequently, a system of surface vortices exists also.

Table I

No. of sample	Recrystallization annealing		Aging		Phase composition		
	t, °C	τ, hrs	t, °C	τ, hrs	β phase	ω phase	α phase
1	800	1	—	—	+	+	—
2	800	1	390	1	+	+	—
3	800	1	390	3	+	+	—
4	800	1	800	10	+	+	+
5	800	1	500	1	+	—	+
6	800	1	500	8	+	—	+
7	800	1	500	10	+	—	+
8	800	1	500	14	+	—	+
9	800	1	500	16	+	—	+
10	800	1	500	56	+	—	+
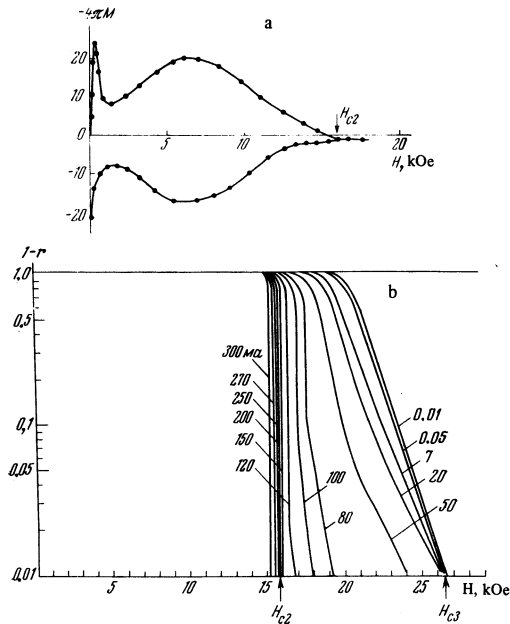
FIG. 1. Method of determination of the critical fields H_{c2} and H_{c3}: a—magnetization curve, M is in arbitrary units; b—curves of reduced resistance for various values of the transport current; $r = R/R_n$—reduced resistance of the sample. The external magnetic field is parallel to the transport current. Sample No. 2, T = 0.88 T_c.

FIG. 2. Effect of the ω phase on the dependence of the critical surface current density on the intensity of the magnetic field (T = 0.9T_c); ●—sample No. 1; ○—sample No. 2; △—sample No. 3; □—sample No. 4.

measured current density j = 1 A/cm^2. The average width of the transition was equal to 0.1°K. The temperature for which R = 0.5R_n was taken to be T_c.

2. EFFECT OF THE STRUCTURE OF THE ALLOY ON THE VALUE OF THE CRITICAL CURRENT OF SURFACE SUPERCONDUCTIVITY

The change in the structural state of the alloy Ti–22 at.% Nb leads to a change in practically all its superconducting properties. The critical surface current undergoes the most significant change. This is due to the increase in the pinning force on particles of the second phase.

Figure 2 shows the density of the critical surface current as a function of the external magnetic field for samples containing particles of the ω phase (of steadily increasing size) uniformly distributed over the volume. For sample No. 1, the dimensions of the ω particles were less than 50 Å, the second critical field was H_{c2} = 8.2 kOe and the surface critical current was less than 0.01 A/cm. An increase in the time of heat treatment leads to an increase in the dimensions of the ω particles—the second critical field H_{c2} and the surface critical current also increase correspondingly.

Such an effect of the α phase on the value of the surface critical current and the critical fields H_{c2} and H_{c3} has also been studied. Here we observed the same tendency: increase in H_{c2} and j_{cr} for increase in the aging time. Sample No. 6 has a critical field H_{c2} twice that of the recrystallized sample No. 1. Such big particles were precipitated for sample No. 10, which was heat treated for 56 hours at a temperature of 500°C, that the critical current began to decrease.

The results of the investigation of the dependence of $j_{cr}(H)$ on the structure can be explained qualitatively

by use of the model of a rigid vortex lattice.[8] According to this model a state with a non-zero surface current can be created only by pinning the vortex lattice. The role of the pinning centers of the vortices is played by structural defects. In our case, these are particles of the ω and α phases, which have a critical temperature lower than the T_c of the matrix. The value of the current is determined by the value of the pinning force, which is in turn determined by the values of the concentration and composition of the particles of the nonsuperconducting phase. With increase in annealing time of the particle s, the concentration and the dimensions of the particles increase. Here an increase is observed in the critical surface current. In samples No. 4 and 9, where the particles are large and numerous, the critical current corresponds to the limiting theoretical value calculated from the formula of Abrikosov.[9] The pinning force in them is so large that the destruction of superconductivity takes place not under the action of the Lorentz forces but upon achievement of the critical velocity by the superconducting condensate. For example, for sample No. 4, the theoretical value of the density of the critical current in the field H_{c2} is equal to 1.7 A/cm, while its experimental value is 2 A/cm.

3. TEMPERATURE DEPENDENCE OF THE CRITICAL FIELDS H_{c2} AND H_{c3} AND THE EFFECT OF THE STRUCTURE OF THE ALLOY ON T_c, κ, AND ρ_n

The values of the critical fields H_{c2} and H_{c3} also depend strongly on the dimensions and the concentration of the ω particles. An increase in the aging time leads to growth in the fields H_{c2} and H_{c3}. Table II characterizes the growth of the critical fields H_{c2} and H_{c3} of samples No. 2, 3, and 4 in comparison with the

Table II

No. of samples	$H_{c2}(t)/H_{c2}^*(t)$	$H_{c3}(t)/H_{c3}^*(t)$
2	1.52	1.25
3	1.66	1.60
4	2.03	2.15

critical fields H_{c2}^* and H_{c3}^* of the recrystallized sample No. 1. It is seen that for the sample No. 4 with a rigidly pinning Abrikosov vortex lattice[8] the fields H_{c2} and H_{c3} are about twice as large over the entire measurement range of temperature as for the sample No. 1. Such a behavior is connected with the enrichment of the matrix by niobium.

From the GLAG theory[10] it follows that for alloys ($l \ll \xi$)

$$H_{c2}(0) = 2.6 \cdot 10^4 \rho_n \gamma T_c \quad \text{(for } T = 0\text{)}, \tag{2}$$

$$(dH_{c2}/dt)_{t=1} = 3.8 \cdot 10^4 \rho_n \gamma T_c, \tag{3}$$

where γ is the coefficient for the linear term of the electron specific heat, which is equal in our alloy to 7.65×10^3 erg/cm^3-deg^2, ρ_n is the electric resistivity in the normal state in ohm-cm.

In the absence of Pauli paramagnetism the theory of Werthamer et al.[11] gives the following value of the critical field H_{c2} for alloys for T = 0:

$$H_{c2}(0) = 0.693 (dH_{c2}/dt)_{t=1}. \tag{4}$$

The effect of the Pauli paramagnetism on $H_{c2}(0)$ can be estimated by using the Maki formula[12]

$$H_{c2}^*(0) = \frac{H_{c2}(0)}{(1+\alpha^2)^{1/2}}, \quad \alpha = \sqrt{2}\frac{H_{c2}(0)}{H_p(0)}; \quad H_p(0) = 18400 T_c. \tag{5}$$

The experimental values of $(dH_{c2}/dt)_{t=1}$, and also the values of $H_{c2}(0)$ and $(dH_{c2}/dt)_{t-1}$, computed from equations (2)—(5), are given in Table III.

It is seen from the table that the extrapolated values of $H_{c2}(0)$ are in satisfactory agreement with the values of $H_{c2}^*(0)$ calculated from (4) and (5). The experimental values of the slope $(dH_{c2}/dt)_{t=1}$ of samples No. 2—4 are 20% higher than the theoretical values calculated from the GLAG theory.

The connection of the structure of the alloy Ti = 22 at.% Nb with its superconducting parameters is summarized in Table IV. In the calculation of H_c, λ, ξ, and κ the following formulas were used:

$$H_c = T_c \sqrt{2\pi\gamma}\left[1 - \left(\frac{T}{T_c}\right)^2\right], \quad \lambda(T) = \sqrt{\frac{\Phi_0 H_{c2}}{4\pi H_c^2}},$$

$$\xi(T) = \sqrt{\frac{\Phi_0}{2\pi H_{c2}}}, \quad \kappa_{theor} = \frac{\lambda(T)}{\xi(T)}, \tag{6}$$

$$\kappa_{exp} = 7.5 \cdot 10^3 \gamma^{1/2}\rho_n.$$

The gradual increase of T_c of samples No. 2, 3, and 4 is connected with the fact that the superconducting matrix is enriched with niobium in the increase in ω particles. For a similar reason, T_c increases in the series of samples containing the α phase; from 7.94°K in sample No. 5 to 9.32°K in sample No. 10. Enrichment of the matrix with niobium in the aging process leads to a decrease in the free path length. As a consequence, the resistivity and the parameter κ increase with growth in the ω ellipsoids. The critical fields H_{c2} and H_{c3} also increase proportionally.

Table III

No. of sample	T_c, °K	T = 0.9 T_c					κ_{theor}	κ_{exp}	ρ_n, $\mu\Omega$-cm
		H_c, Oe	H_{c2}, kOe	H_{c3}, kOe	λ, Å	ξ, Å			
1	7.39	304	8,2	18,6	3800	200	19	26	40
2	7.41	310	12,8	22,9	4600	160	28	29.5	45
3	7.85	325	13,8	30	4550	150	30	32	49
4	8.26	340	17,0	37	4800	140	34	36	55

Table IV

No. of sample	$(dH_{c2}/dt)_{t=1}$		$H_{c2}(0)$, kOe		$H_{c2}^*(0)$, kOe		$H_{c2}(0)$, kOe
	Experimental value	by Eqs. (2) and (3)	by Eq. (2)	by Eq. (4)	by Eqs. (2) and (5)	by Eqs. (4) and (5)	Parabolic extrapolation
1	84	84	59	58	51	50	42
2	126	97	66	87	55	65	63
3	138	112	77	96	62	70	69
4	168	132	91	116	70	86	84
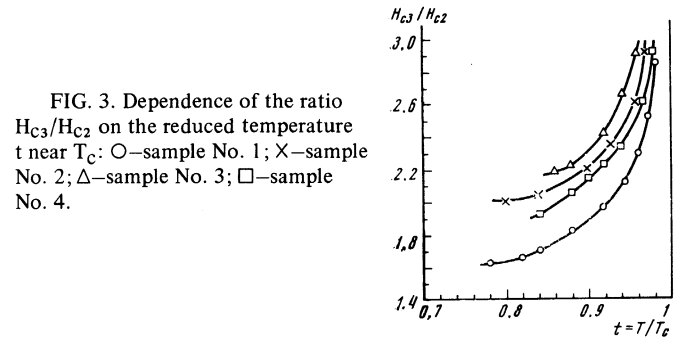
FIG. 3. Dependence of the ratio H_{c3}/H_{c2} on the reduced temperature t near T_c: O—sample No. 1; ×—sample No. 2; △—sample No. 3; □—sample No. 4.

4. TEMPERATURE DEPENDENCE OF THE RATIO H_{c3}/H_{c2} NEAR T_c

Figure 3 shows the experimental values of $H_{c3}(t)/H_{c2}(t)$ of samples 1—4. It is seen that the value of the ratio H_{c3}/H_{c2} is greater than 1.69 in the temperature range $0.8 T_c < T \lesssim T_c$ for all the samples, and that this ratio increases upon approach to T_c.[2] The error in the determination of the ratio H_{c3}/H_{c2} was of the order of 10%.

The increase in the ratio H_{c3}/H_{c2} near T_c can be explained if we assume that the surface layer at a critical temperature T_c greater than the critical temperature of the bulk of the sample.[14] Actually, linear extrapolation of $H_{c3}(t)$ to H = 0 in the region t = 1 has shown that all the samples have a critical temperature $T_{c3} > T_c$. Sample No. 1 had the greatest difference $T_{c3} - T_c = 0.02$°K.

We now carry out a quantitative comparison of our data with the theory of[15]. According to this theory, the BCS pairing potential (V_0) changes by an amount δV_0 in a surface layer of thickness D. The change in the pair potential brings about a change in the critical temperature of the surface of the sample:

$$\frac{\delta T}{T_c} = \frac{T_{c3} - T_c}{T_c} = \frac{1}{N(0)V_0}\frac{\delta V}{V_0}, \tag{7}$$

where $N(0)$ is the density of electron states on the Fermi surface.

---

[2] A similar result was observed by Khukhareva and Goncharov [13] on the alloy Nb-80% Zr.
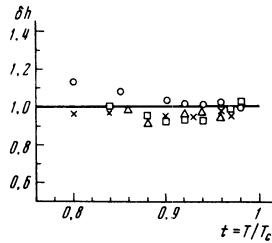
FIG. 4. Comparison of the experimental dependence of δh with the theory of [15]: X—sample No. 1; O—sample No. 2; $\triangle$—sample No. 3; $\square$—sample No. 4.

For a quantitative estimate of the ratio, we consider the case in which the thickness of the layer on the surface $D \gg \xi$, inasmuch as in our measurements $H_{c3}(T)$ remains linear to $T = 0.995T_C$. Then

$$\frac{H_{c3}}{H_{c2}}(t) = C(T)\left\{ 2\frac{\delta T}{T_c} + \frac{1 + \delta T/T_c - t}{(1 + \delta T/T_c)(1 - t)}\right\}, \qquad (8)$$

where $C(T) \approx 1.69$ is a coefficient that is weakly temperature dependent.

Figure 4 shows the dependence δh
$= (H_{c3}/H_{c2})_{\text{theor}}/(H_{c3}/H_{c2})_{\text{exp}}$, where $(H_{c3}/H_{c2})_{\text{theor}}$ is computed from Eq. (8). It is seen that there is agreement between our experimental data and the theory of[15]. In order to estimate the thickness of the layer, we assume that $T_{\max} = 0.995\ T_C$ is the temperature of the transition to the second case in the theory of[15], when $D \sim \xi$, We then have

$$\begin{aligned} D &\approx 1.185\xi(T_{max}) \\ &= 1.185 \cdot 0.85\xi(0)(1 - t)^{-1/2}, \end{aligned} \qquad (9)$$

where $\xi(0) = 50$ Å. It follows from (9) that $D \approx 14\ \xi(0)$.

5. TEMPERATURE DEPENDENCE OF THE CRITICAL CURRENT, THE ANISOTROPY OF THE CRITICAL CURRENT, AND THE ANGULAR DEPENDENCE OF THE CRITICAL FIELD H_{c3}

Figure 5 shows the dependence of the critical current density j_{cr} of sample No. 3 on the reduced temperature t. It is seen that, near T_C, the value of $j_{cr}(t)$ has an exponential character (see the lower curve). The upper curve demonstrates the smooth transition from the linear dependence to the exponential. Insofar as we know, such a character of the temperature dependence of j_{cr} is observed here for the first time.

A number of curves of the dependence of the critical current density j_{cr} on the external magnetic field H were recorded for sample No. 9 at $T = 8.18°K$. To each curve there corresponded a fixed value of the angle θ. It has been shown that the curve $j_{cr}(H)$, which corresponds to the angle $\theta = 70°$, for $H > H_{c2}$, lies between the curves of $j_{cr}(H)$ for the angle θ equal to 90 and 45°. Thus, $j_{cr}(H)$ for $\theta = 90°$ is greater than $j_{cr}(H)$ for $\theta = 45°$ or $\theta = 70°$. Figure 6a demonstrates the anomalous angular dependence of the critical current of surface superconductivity: the critical current of samples No. 6—9 increases, when $\theta \gtrsim 45°$. The critical current of samples No. 5 and 10, which have very large and very coarse particles, respectively, of α phase, decreases monotonically with increase in the angle θ (Fig. 6b).

In order to find out whether the effect is due to the surface superconductivity or to phenomena inside the sample in the boundary layers between the α and ω phases, we coated the greater part of the surface of the
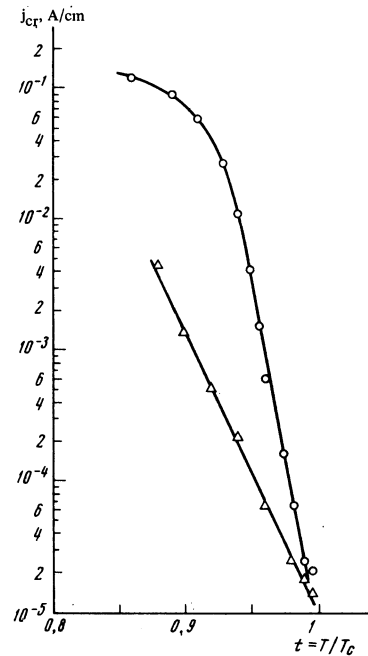
FIG. 5. Temperature dependence of the critical surface current density near T_C of sample No. 3: $\triangle$—external magnetic field $H = 0.75\ H_{c3}$: O—external magnetic field $H = 0.65\ H_{c3}$.
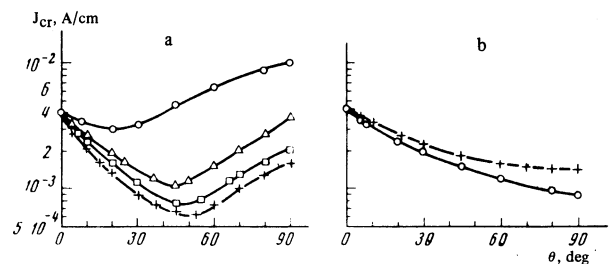
FIG. 6. Angular dependence of the critical current ($T = 0.9\ T_C$; $H = 1.35\ H_{c2}$): a—O—sample No. 6, $H = 21.5$ kOe; $\triangle$—sample No. 7, $H = 28.2$ kOe; $\square$—sample No. 8, $H = 27.9$ kOe; +—sample No. 9, $H = 22.8$ kOe; b—+—sample No. 10, $H = 22.7$ kOe, O—sample No. 5, $H = 18.8$ kOe.
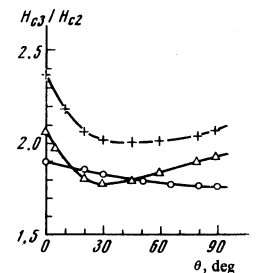
FIG. 7. Angular dependence of the ratio H_{c3}/H_{c2} for $T = 019\ T_C$; +—sample No. 6; $\triangle$—sample No. 9; O—sample No. 10.

strip with pure indium and plotted $j_{cr}(H)$ for two orientations of the strip: $\theta = 0°$ and $\theta = 90°$. It turned out that in the case $\theta = 90°$, there is a weak surface superconductivity, due to the presence of small uncoated portions close to the potential contacts and the edges of the strip. Thus, the anomaly is connected with the surface of the sample.

Figure 7 shows the anomalous dependence of the critical field H_{c3}/H_{c2} on the angle θ, which is expressed as follows: 1) the initial slope of the curve

$H_{C3}(\theta)/H_{C2}$ is equal to 40° for sample No. 9, and 60° for sample No. 6; theoretically, the calculated value of the slope of the curve $H_{C3}(\theta)/H_{C2}$ is equal to 22°;[4] 2) the value of the critical field H_{C3} of samples No. 6 and 9 increases when $\theta \gtrsim 30°$; 3) the value of the ratio H_{C3}/H_{C2} of samples No. 6 and 9 remains anomalously large in comparison with the theoretical value, which is equal to 1.69.

In conclusion, it should be noted that the reason for the anomalous dependence of $j_{cr}(\theta)$ and $H_{C3}(\theta)$ is evidently one and the same. So far as the reason for the exponential temperature dependence of j_{cr} close to T_c, it has not been established.

[1]V. R. Karasik and V. G. Vereshchagin, Zh. Eksp. Teor. Fiz. **59**, 36 (1970) [Sov. Phys.-JETP **32**, 20 (1971)].

[2]V. R. Karasik, V. G. Vereshchagin, and G. T. Nikitina, Kratkie soobshcheniya po fizike (Short Communications in Physics) Phys. Inst., USSR Acad. Sciences, No. 5, 1970.

[3]I. O. Kulik, Zh. Eksp. Teor. Fiz. **55**, 889 (1968) [Sov. Phys.-JETP **28**, 461 (1969)].

[4]S. Sh. Akhmedov, V. R. Karasik, and A. I. Rusinov, Zh. Eksp. Teor. Fiz. **56**, 444 (1969) [Sov. Phys.-JETP **29**, 243 (1969)].

[5]N. V. Zavaritskii, PTÉ No. 2, 1956, p. 140.

[6]N. N. Buinov, Yu. F. Bychkov, V. G. Vereshchagin, V. R. Karasik, G. B. Kurganov, and V. A. Mal'tsev, Fiz. Met. Metalloved. **30**, 754 (1970).

[7]V. Brammer and C. Rhodes, Philos. Mag. **16**, 477 (1967).

[8]Yu. F. Bychkov, V. G. Vereshchagin, V. R. Karasik, G. B. Kurganov, and V. A. Mal'tsev, Zh. Eksp. Teor. Fiz. **56**, 505 (1969) [Sov. Phys.-JETP **29**, 505 (1969)].

[9]A. A. Abrikosov, Zh. Eksp. Teor. Fiz. **47**, 720 (1964) [Sov. Phys.-JETP **20**, 480 (1965)].

[10]P. DeGennes, Superconductivity of Metals and Alloys, Benjamin, 1965.

[11]N. R. Werthamer, E. Helfand, and P. Hohenberg, Phys. Rev. **147**, 295 (1966).

[12]K. Maki, Physics (N.Y.) **1**, 127 (1964).

[13]I. S. Kukhareva and I. N. Goncharov, Preprint, Joint Institute of Nuclear Research R-8-5733, Dubna, 1971.

[14]H. Fink and W. Joiner, Phys. Rev. Lett. **23**, 120 (1969).

[15]Chia-Ren Hu, Phys. Rev. **187**, 574 (1969).